Materials Transactions, Vol. 48, No. 9 (2007) pp. 2483 to 2488

Effect of Die Surface Roughness on Deformation Characteristics and Cavitation during Blow Forming in a Superplastic 5083 Alloy

Horng-yu Wu[1], Chui-hung Chiu[1], Shyh-hung Sheu[1], Shyong Lee[2] and Jian-yih Wang[3]

[1]*Institute of Engineering Science, Chung-hua University, HsinChu 30012, Taiwan, R. O. China*
[2]*Department of Mechanical Engineering, National Central University, Jhongli, Taoyuan 32001, Taiwan, R. O. China*
[3]*Department of Materials Science and Engineering, National Dong Hwa University, Shou-Feng, Hualien 97401, Taiwan, R. O. China*

Effect of die surface roughness on deformation behavior of a superplastic material has relatively been less examined, though it is important for industrial application during die design. In this paper, a superplastic 5083 Al alloy under bi-axial deformation was investigated by deforming the sheet into a rectangular die cavity with different degrees of die surface roughness. It was found that reducing the interfacial friction by use of a die with a smaller surface roughness improved the metal flow after the deformed sheet had made contact with the die bottom surface. Changes of the metal flow during forming not only developed a better thickness distribution of the formed part, but also reduced the cavitation levels. [doi:10.2320/matertrans.MRA2006319]

(Received November 6, 2006; Accepted June 14, 2007; Published July 25, 2007)

Keywords: *superplastic forming, superplastic 5083 aluminum alloy, surface roughness, cavitation*

1. Introduction

Internal cavities are commonly observed during superplastic deformation in most alloys, and extensive cavitation may lead to premature failure or result in a finished part with degraded mechanical properties.[1)] A considerable amount of research has been performed to study the characteristics of cavitation during superplastic deformation.[2–15)] However, most of the studies explored cavitation by use of a tensile test, these studies might not provide enough information for industrial application. Since die surface finish must be specified to manufacture a forming die, the effect of die surface roughness has not yet been taken into account in the cavitation analysis.

During complex superplastic part forming, the surface friction of the die will limit the following deformation of the overlaid region, if the friction is large, and thinning is localized in the region where contact has not been made resulting in a greater strain in the last formed areas. The strain, strain rate, and stress state can vary widely in different regions of the formed part,[16–18)] causing variable cavitation levels from one location to another. Provided that the interfacial friction is reduced by using a die with a smaller surface roughness, the thinning gradient would be reduced, since continued metal flow might be possible for the overlaid region after die contact. Consequently, using a die with a smaller surface roughness during superplastic forming not only could improve the thickness distribution of the formed parts, but also would influence the cavitation levels in the formed part.

In order to meet the need for industrial application it is necessary to understand the effect of die surface roughness on the cavitation behavior under multiaxial deformation during superplastic forming. The work presented here evaluates the influence of die surface roughness on the superplastic deformation characteristics of a superplastic (SP) 5083 Al alloy under bi-axial strain deformation. Gas pressure forming was conducted to deform the sheets into a die with a rectangular cavity. Focus was placed on the metal flow and evolution of cavitation during deformation.

2. Material and Experimental Procedures

2.1 Material and preparation

Sky Aluminum Company, Japan, provided the SP5083 alloy sheet. The analyzed chemical composition was (mass%) Al-4.6Mg-0.67Mn-0.1Cr-0.02Cu-0.05Si- < 0.05Fe- < 0.01Ti. An ingot of the alloy was homogenized at 530°C for 8 h and hot rolled to a thickness of 6 mm followed by cold rolling to a thickness of 2.0 mm. The sheet was recrystallized at 400°C for 10 min resulting in an average grain size of 8.6 μm before superplastic deformation.

Grid circles of diameter d_o (2.5 mm) etched on the sheets were used to measure strain levels in each test. During forming the etched circles were distorted into ellipses and/or larger circles, and these deformed grid circles were used to measure strain levels in each case. Measurements of the major (d_1), minor (d_2) diameters and thickness (h_1) after deformation were made to determine the principal strains. The principal strains, effective strains and strain rates can then be expressed as:

$$\varepsilon_1 = \ln(d_1/d_o) \quad (1)$$

$$\varepsilon_2 = \ln(d_2/d_o) \quad (2)$$

$$\varepsilon_3 = \ln(h/h_o) \quad (3)$$

$$\bar{\varepsilon} = \left[(2/3)\left(\varepsilon_1^2 + \varepsilon_2^2 + \varepsilon_3^2\right)\right]^{1/2} \quad (4)$$

$$\dot{\bar{\varepsilon}} = \bar{\varepsilon}/t \quad (5)$$

Where
h_o: Original thickness of the sheet
h: Thickness of the deformed sheet
$\varepsilon_{1,2,3,}$: Principal strain in direction 1, 2 and 3
$\bar{\varepsilon}$: Effective strain
$\dot{\bar{\varepsilon}}$: Effective strain rate
t: Forming time

2.2 Superplastic plastic forming tests

The superplastic sheet was formed into a rectangular die cavity by compressed argon gas. The die had a cavity of 120 mm (length) × 40 mm (width) × 20 mm (depth). The dies were made of medium-carbon low alloy steel 4340 with the values of surface roughness Ra = 0.48 and 1.74 μm. Incremental step strain rate tensile tests were first conducted covering the range of strain rates from $5 \times 10^{-5}\,s^{-1}$ to $1 \times 10^{-2}\,s^{-1}$ to determine the superplastic flow characteristics. The variation of strain rate sensitivity index m ($m = d\log\sigma/d\log\dot{\varepsilon}$), over a wide rage of strain rates, with strain was determined by using separate specimens strained to various amounts prior to the step strain rate test. The pressure profiles for the desired strain rates were calculated by the computer program SUPFORM2[19] using the material constant and m values obtained from the tensile tests. Test runs were also made to modify the pressure profile predicted by the computer program in order to achieving the desired strain rate. Gas pressure forming was performed at 525°C and at strain rates of $1 \times 10^{-3}\,s^{-1}$ and $2 \times 10^{-4}\,s^{-1}$. Several interrupted tests were performed to bulge the sheets to various depths for each strain rate, the deformed sheets were then utilized to evaluate the effect of strain on cavitation. In order to obtain the fundamental information on the characteristics of cavity development in SP5083 Al alloy, lubricant and back pressure were not used in this study.

2.3 Metallographic inspection

Optical microscopy was used to inspect cavitation of the test piece. The specimens for metallographic examination were mechanically polished and then slightly etched to remove smeared metal covering the cavities. Cavity area fractions were measured by computer imaging equipment and calculated by using OPTIMAS 5 software.[20] The optical image was first converted into a binary video image. The number of pixels in the cavity (black area) were counted and divided by the total number of pixels in the image to obtained cavity area fraction.

3. Results and Discussion

3.1 Forming into a die with a rectangular cavity

The deformation characteristics for bulging a sheet into a die cavity with a simple geometry could be considered to separate into two stages.[21] In stage I, the sheet will deform freely as part of a hemi-cylindrical shape for forming a rectangular pan until its central point touches the bottom surface of the die. The second stage starts when the deformed sheet just touches the bottom surface of the die. In the second stage, the sheet is overlaid on the bottom surface and on the sidewall surface as the deformation proceeds, the surface condition of the die will affect the subsequent deformation and the thinning effect of the overlaid region.

Figure 1 illustrates the deformation contour and particle path of the deformed sheets for forming with a die surface roughness of 1.74 μm. After the deformed sheet makes contact with the die bottom surface, surface friction of the die restricts the metal flow to prevent thinning of the overlaid region. Metal flow moves from the bottom center and the side wall toward the location near the bottom

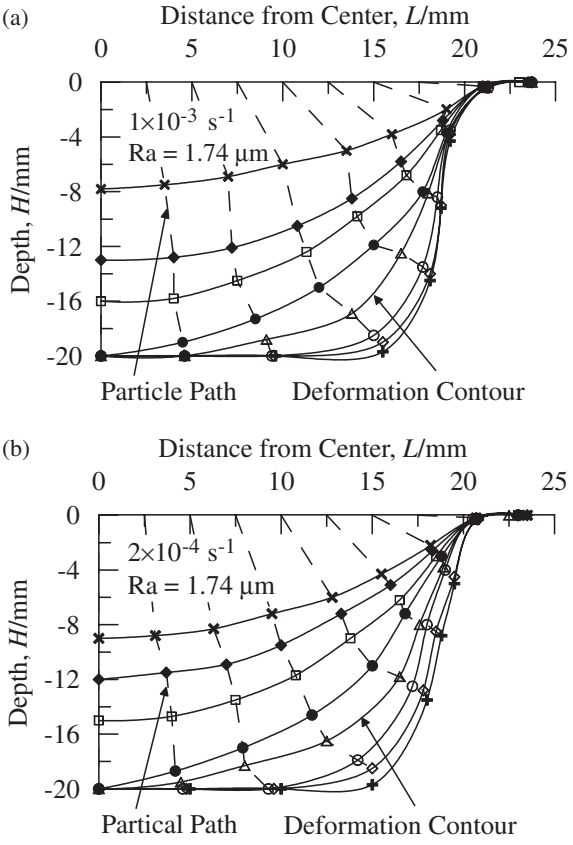

Fig. 1 Deformation contour and particle path of the sheet during deformation for forming into a die with a surface roughness of 1.74 μm at two different strain rates. (a) $1 \times 10^{-3}\,s^{-1}$, (b) $2 \times 10^{-4}\,s^{-1}$.

corner. In the later stage of forming, the free deformed region of the sheet is responsible for the major thinning effect, the bottom corner is usually the location where the thinnest region of the formed part is located. Figure 1(a) shows that the sheet almost sticks to the bottom surface of the die after contact is made for forming at a strain rate of $1 \times 10^{-3}\,s^{-1}$. However, sticking of the particle path of the overlaid region was not presented for forming at a lower strain rate of $2 \times 10^{-4}\,s^{-1}$, as shown in Fig. 1(b). A small amount of displacement of metal flow takes place after the deformed sheet touches the bottom surface. Since the imposed pressure in the later stage for forming at a strain rate of $2 \times 10^{-4}\,s^{-1}$ is about 0.20 MPa, which is small than that of 0.70 MPa for forming at a strain rate of $1 \times 10^{-3}\,s^{-1}$. A lower imposed pressure during forming resulting in a lower friction force for the overlaid region causes the variation of the metal flow after the deformed sheet has overlaid on the bottom surface of the die.

The deformation contour and particle path for forming with a die surface roughness of 0.48 μm at two different strain rates are depicted in Fig. 2. A smaller die surface roughness reduces the surface friction between the deformed sheet and bottom die surface, some displacement of metal flow could be observed for the overlaid region for both forming rates. Although the metal flows are similar for using the dies with different degrees of surface roughness, forming carried out with a smaller die surface roughness improves the metal flow in the later stage of forming. Figure 2 also indicates that

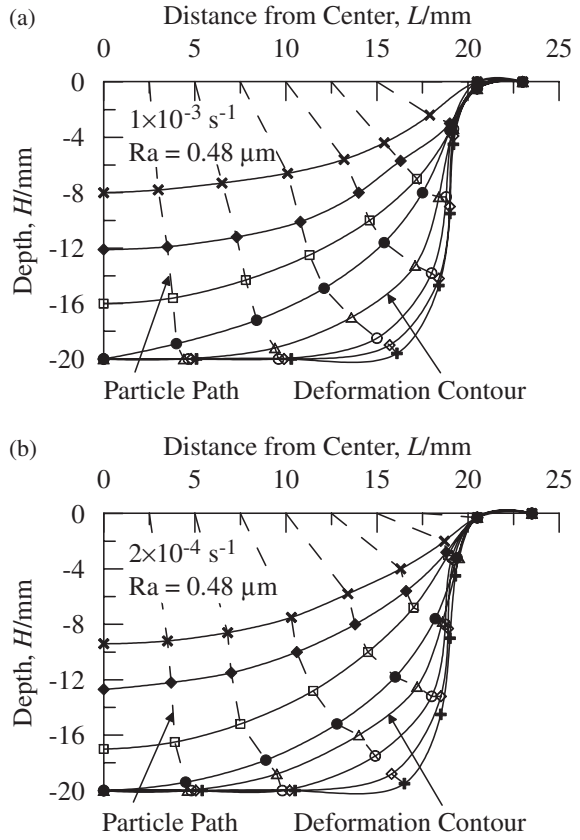

Fig. 2 Deformation contour and particle path of the sheet during deformation for forming into a die with a surface roughness of 0.48 μm at two different strain rates. (a) $1 \times 10^{-3}\,s^{-1}$, (b) $2 \times 10^{-4}\,s^{-1}$.

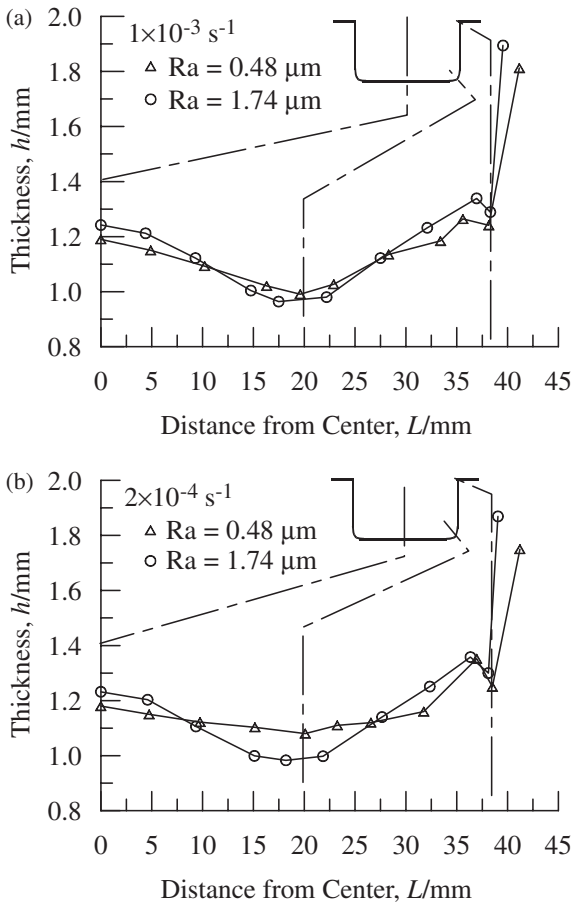

Fig. 3 Thickness distribution along the transverse cross section of the completely formed rectangular pan formed at two different strain rates showing the effect of die surface roughness. (a) $1 \times 10^{-3}\,s^{-1}$, (b) $2 \times 10^{-4}\,s^{-1}$.

forming with a smaller die surface roughness at a lower strain rate exhibits greater displacement of the overlaid region as that for forming with a greater die surface roughness.

3.2 Thickness distribution

The effect of die surface roughness on the thickness distribution of the completely formed rectangular pans is demonstrated in Fig. 3. For forming with a greater die surface roughness of 1.74 μm, the interfacial friction is large, when the sheet makes contact with the die surface, the deformation in that contact area is restricted, and thinning is localized in the non-contact areas resulting in a greater degree of thinning gradient. Major thinning effect takes place at the non-contact regions of the sheet in the later stage of forming, the thinnest positions are around 17.5 and 18.2 mm away from the bottom center of the completed formed pans for forming at strain rates of $1 \times 10^{-3}\,s^{-1}$ and $2 \times 10^{-4}\,s^{-1}$, respectively. The thinnest locations do not exactly presented at 20 mm away from the bottom center due to the design of the die, the die has a draft of 5° with a die entry radius of 3 mm causing these variations.

If the interfacial friction is reduced, as the case where a die with a smaller surface roughness of 0.48 μm is used, the thinning gradient of the formed part will be reduced; as displayed in Fig. 3, since continued metal flow after die contact is possible. The thinnest locations fall at the positions about 19.6 and 20.1 mm away from the bottom center for forming at strain rates of $1 \times 10^{-3}\,s^{-1}$ and $2 \times 10^{-4}\,s^{-1}$, respectively. It is also noticed that greater localized thinning appears at the die entry region for forming with a smaller die surface roughness. The nonuniformity of the thickness distribution could be improved by using a die with a smaller surface roughness and forming at a lower strain rate.

The changes of the thickness distribution due to die surface roughness can be examined from the actual deformation contour and particle path during deformation; as shown in Figs. 1 and 2. For forming with a greater die surface roughness, after the deformed sheet has been overlaid on the die surface, the metal flows do not move or move a little distance away from the center region, which depends on the imposed pressure (forming rate) during forming. Although thinning at the bottom corner in the final stage pulls the material moving toward this region, the thinning effect is still more significant at the bottom corner. Therefore, the bottom corner is the thinnest position of the formed pans. For forming with a smaller die surface roughness, the material still moves some distance from the bottom center toward the side wall after the deformed sheet has been overlaid on the die surface. The thinning effect of the deformed sheet keeps on taking place in the overlaid regions during the whole forming process, which results in the thinnest position to be shifted a little distance away from the bottom center.

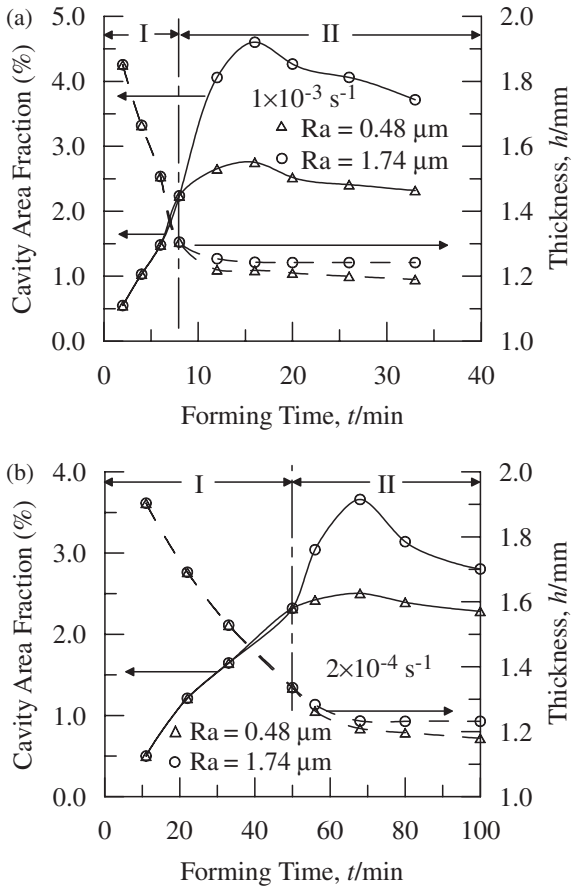

Fig. 4 Evolution of cavity area fraction and thickness at the central region of the formed pan versus forming time at two different strain rates showing the effect of die surface roughness. (a) 1×10^{-3} sec^{-1}, (b) 2×10^{-4} sec^{-1}.

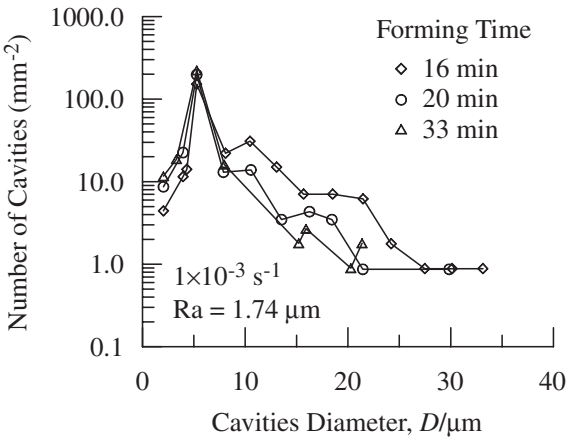

Fig. 5 Number of cavities per unit area versus cavity diameter at various forming time formed with a die surface roughness of 1.74 μm at a strain rate of 1×10^{-3} s^{-1}.

3.3 Cavitation

Figure 4 displays the evolution of cavity area fraction and the thickness at the central region of the deformed sheet with forming time. For forming at a strain rate of 1×10^{-3} s^{-1}, the center of the sheet touched the bottom surface at around 8 min, and it took about 33 min for completely forming a rectangular pan, as shown in Fig. 4(a). Hence, the time span from 8 to 33 min accounts for the deformation of stage II. In this stage, the cavity area fraction of the central region keeps on increasing in the early stage, it reaches a maximum value at a forming time around 16 min, then it decreases till the end of forming. The variation of cavity area fraction with time in stage II could be associated to the thinning behavior of the sheet. The thickness of the central point decreases with increasing forming time, it reaches a thickness about 1.24 mm at a forming time around 16 min and then remains almost as a constant for forming with a greater die surface roughness of 1.74 μm. The cavity area fraction increases with decrease in thickness in the early stage of stage II, it begins to decrease as significant thinning of the deformed sheet brings to an end.

It is believed that cavity closure occurs to cause the decrease in cavity area fraction in the later stage of forming while the sheet has been overlaid on the die surface.[21] Decrease in cavity area fraction could be related to the cavity shrinkage as a result of sintering effect. After the significant thinning of the deformed sheet is prevented by the restriction of the surface friction, decrease in cavity area in the region at which significant thinning does not occur could be described as the sintering of cavities at elevated temperature under pressure.[22] A plot of the number density of cavities as a function of cavity size forming at a strain rate of 1×10^{-3} s^{-1} is given in Fig. 5 to illustrate the effect of the cavity shrinkage in the later stage of forming. The decrease of the high-radius tail with increasing forming time indicates that cavity shrinkage does take place. The density for the smallest cavity size (~2 μm) also appears to increase with forming time. Since the thickness at the central region almost remains as a constant in the later stage of forming, no significant deformation is observed, increase in the number density of the smallest cavity should not be resulted from cavity nucleation. Micrographs in the later stage of forming showing the progression of cavitation of the pans from the central locations formed at a strain rate of 1×10^{-3} s^{-1} are given in Fig. 6. It is also seen in the micrographs that the number of the small-sized cavity increases and the size of the large cavity decreases, as forming proceeds from 16 to 33 min.

Since metal flow is possible after the sheet overlaid on the die surface for forming with a smaller die surface roughness of 0.48 μm at a strain rate of 1×10^{-3} s^{-1}, thickness of the sheet at the central point keeps on decreasing, no constant thickness with forming time was observed, as shown in Fig. 4(a). Although, the tendency of thickness decreasing becomes sluggish in the later stage of forming, thickness never reaches a significant constant state. Continuously decreasing in thickness during forming thus alters the variation of cavity area fraction with forming time, some cavity shrinkage still takes place in the later stage of forming.

Similar results are also observed for forming at a lower strain rate; as shown in Fig. 4(b). The deformed sheet comes into contact with the bottom surface of the die at a forming time around 50 min for forming at a strain rate of 2×10^{-4} s^{-1}. The maximum cavity area fraction occurs at the forming time about 68 min, this is also the time that significant thinning of the sheet stops for forming with a die surface roughness of 1.74 μm. It reaches a thickness about

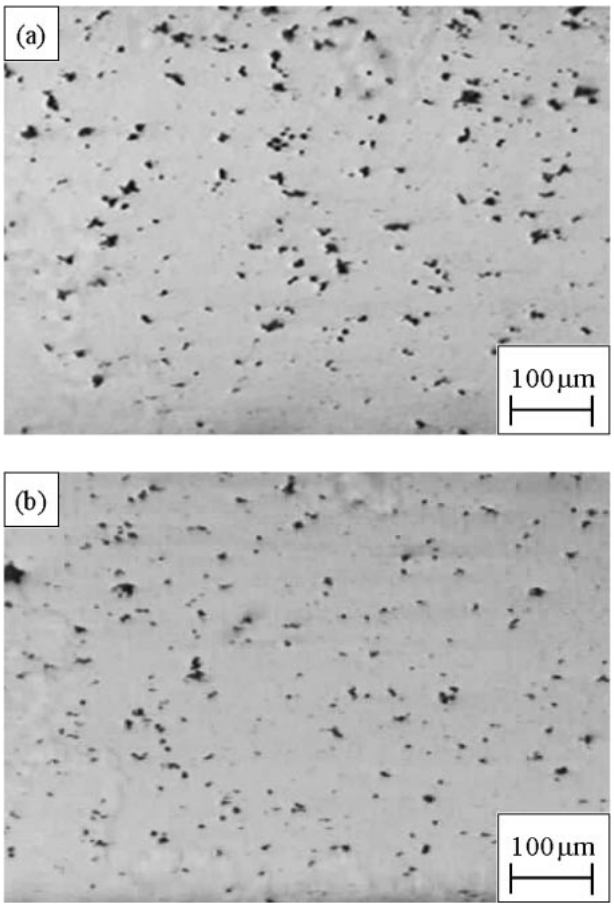

Fig. 6 Micrographs showing the progression of cavitation at the central region of the pans formed with a die surface roughness of 1.74 μm at a strain rate of $1 \times 10^{-3}\,s^{-1}$. (a) Forming time = 16 min, (b) Forming time = 33 min.

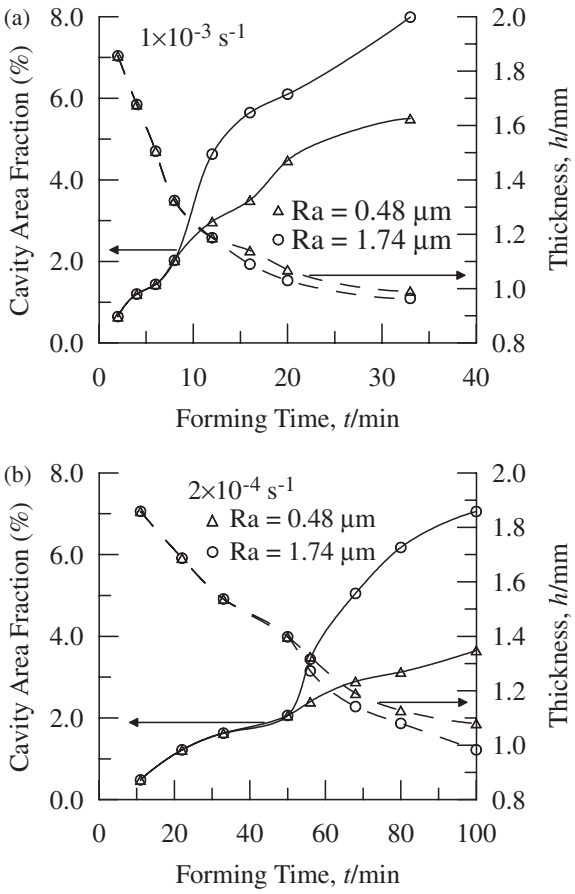

Fig. 7 Evolution of cavity area fraction and thickness at the latest formed region versus forming time at two different strain rates showing the effect of die surface roughness. (a) $1 \times 10^{-3}\,s^{-1}$, (b) $2 \times 10^{-4}\,s^{-1}$.

1.23 mm and then remains almost as a constant. Continuously decreasing in thickness during forming was also observed for forming with a smaller die surface roughness of 0.48 μm.

Figure 7 illustrates the evolution of cavity area fraction and the thickness with forming time at the bottom corner where is the latest area to contact the die. Since interfacial friction does not influence the thinning effect of the deformed sheet at this region, thickness of the sheet at this area keeps on decreasing as forming proceeds. Therefore, cavity area fraction continues to increase with forming time for both strain rates. These results also reconfirm that the decrease in cavity area fraction at the central region in the later stage of forming is due to cavity shrinkage.

Figure 7 also indicates that the smaller maximum cavity levels and larger values of the thinnest thickness were observed for forming with a smaller die surface roughness. Although die surface roughness does not locally influence the thinning effect of this position, the die surface roughness could change the metal flow during deformation. Using a die with a smaller die surface roughness would improve the thickness distribution of the formed part leading to reductions of cavity levels.

Figure 8 demonstrates the effect of die surface roughness on the cavity distribution along the transverse cross section of the completely formed pans. It shows that the cavity levels could be reduced in the formed parts for forming with a smaller die surface roughness; especially for forming at a lower strain rate. The maximum cavity area fractions for forming at a strain rate of $1 \times 10^{-3}\,s^{-1}$ are 7.99 and 5.50% for forming with the die surface roughness values of 1.74 and 0.48 μm, respectively; it is about 31.16% reduction in cavity area fraction. The maximum cavity level decreases from 7.06 to 3.65% for forming at a lower strain rate of $2 \times 10^{-4}\,s^{-1}$. A reduction of 48.30% was found in this study. Figure 8 also indicates that the locations of the maximum cavity levels shift to the positions toward the side wall of the die due to the effect of using a die with a smaller surface roughness.

4. Conclusions

An analysis of the effect of die surface roughness on deformation characteristics of a SP5083 Al alloy through usage of blow forming was undertaken in the present study. Effect of die surface roughness on cavitation due to bi-axial deformation was analyzed. The following conclusions were determined on the basis of this work.

First, a smaller die surface roughness of 0.48 μm reduced the interfacial friction and changed the metal flow in the later stage of forming, the metal flow moved from the bottom center toward the location near the side wall. Changes of the metal flow during forming improved the thickness and the cavitation distribution along the transverse direction of the

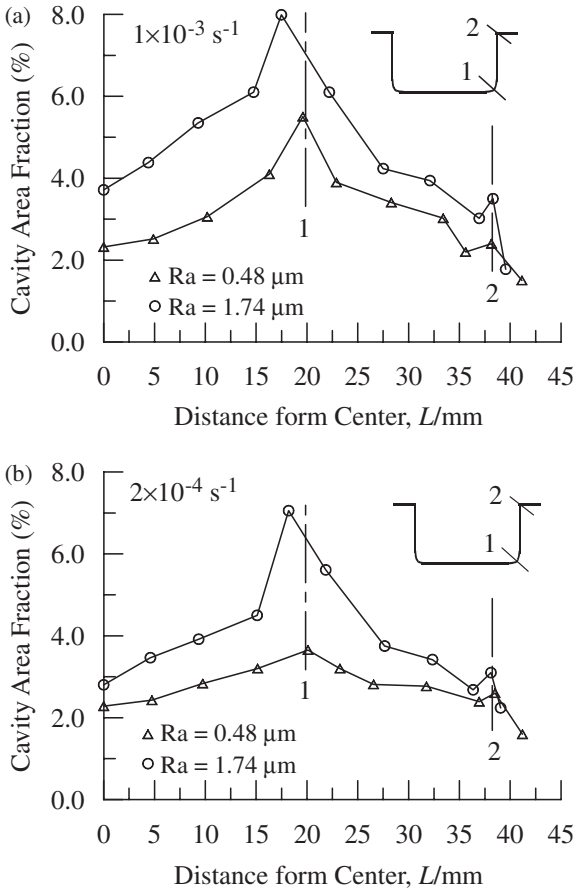

Fig. 8 Cavity area fraction distribution along the transverse cross section of the rectangular pan formed at two different strain rates showing the effect of die surface roughness. (a) $1 \times 10^{-3}\,s^{-1}$, (b) $2 \times 10^{-4}\,s^{-1}$.

formed pans, the locations with thinnest thickness and with maximum cavitation level was shifted to the positions near the side wall. The thinnest regions and the positions with maximum cavitation levels of the parts formed with a smaller die surface roughness located at about 19.6 and 20.1 mm away from the bottom center for forming at strain rates of $1 \times 10^{-3}\,s^{-1}$ and $2 \times 10^{-4}\,s^{-1}$, respectively.

In the second stage of forming, variation of cavity area fraction with forming time in the central region was related to the thinning behavior at his location. For forming with a greater die surface roughness of 1.74 μm, the cavity area fraction increased with decreasing thickness, and it turned to decrease while the thickness of the sheet remained as a constant for both forming rates. Decrease in cavity area fraction was believed to be the result of cavity sintering effect. The effect of cavity shrinkage for forming with a smaller die surface roughness was less obvious due to continuously decreasing in thickness in the later stage of forming.

Finally, the cavity levels could be effectively reduced in the formed parts for forming with a smaller die surface roughness of 0.48 μm. The maximum cavity area fraction was reduced about 48.30% for forming at a strain rate of $2 \times 10^{-4}\,s^{-1}$. The effect of reducing cavity level for forming at a higher strain rate was less than that for forming at a lower strain rate; using a die with a smaller surface roughness caused the maximum cavity level to decrease about 31.16% for forming at a strain rate of $1 \times 10^{-3}\,s^{-1}$.

Acknowledgements

This work was conducted through grant from National Science Council under the contract NSC 93-2212-E-216-005.

REFERENCES

1) C. C. Bampton, A. K. Ghosh and M. W. Mahoney: *Proc. of an International Conference on Superplasticity in Aerospace - Aluminum*, ed. by R. Pearce and L. Kelly, (SIS, Cranfield Institute of Technology, Bedford, England, 1985) pp. 1–35.
2) A. R. Ragab: Mater. Sci. Tech. **21** (2005) 399–407.
3) A. H. Chokshi: Mater. Sci. Eng. A **410–411** (2005) 95–99.
4) P. D. Nicolaou and S. L. Semiatin: Acta Mater. **51** (2003) 613–623.
5) Gouthama and K. A. Padmanabhan: Scripta Mater. **49** (2003) 761–766.
6) H. Y. Wu: J. Mater. Processing Tech. **101** (2000) 76–80.
7) A. K. Ghosh and D. H. Bae: Mater. Sci. Forum **243–245** (1997) 89–98.
8) R. Verma, P. A. Friedman, A. K. Ghosh, C. Kim and S. Kim: J. Mat. Eng. Performance **4** (1995) 543–550.
9) M. G. Zelin, H. S. Yang, R. Z. Valiev and A. K. Mukherjee: Metall. Trans. **A 24A** (1993) 417–424.
10) S. J. Hales, T. T. Bales, W. F. James and J. M. Shinn: *Proc. of Superplastcity in Aerospace II*, ed. by T. R. McNelley and T. C. Heikkenen, (TMS, Warrendal, PA, 1990) pp. 167–185.
11) J. Pilling and R. Ridley: *Proc. of Superplastcity in Aerospace*, ed. by H. Heikkenen and T. McNelley, (The Metallurgical Scoiety, Warrendal, PA, 1988) pp. 183–198.
12) J. Pilling and R. Ridley: Acta Metall. **34** (1986) 669–679.
13) M. J. Stowell, D. W. Liversy and N. Ridley: Acta. Metall. **32** (1984) 35–42.
14) A. C. F. Cocks and M. F. Ashby: Metal Sci. **16** (1982) 465–474.
15) I. W. Chen and A. S. Argon: Acta. Metall. **29** (1981) 1759–1768.
16) M. G. Zelin, S. Guillard and P. K. Chaudhury: Mater. Sci. Forum **243–245** (1997) 137–142.
17) K. S. K. Chockalingam, M. Neelakantan, S. Devaraj and K. A. Padamanabhan: J. Mater. Sci. **20** (1985) 1310–1320.
18) Y. Q. Song and J. Zhao: Mater. Sci. Eng. **84** (1986) 111–125.
19) CEMEF, SUPFORM2 User's guide, Version 1.0, 1989, Fcole des Mines de Paris.
20) Optimas Corporation, Optimas 5 Software, 6th edition, 1995, P.O. Box 24467, Seattle, Washington 98124-0467.
21) H. Y. Wu: Mater. Sci. Eng. A **291** (2000) 1–8.
22) A. Varloteaux, J. J. Blandin and M. Suery: Mater. Sci. Tech. **5** (1989) 1109–1117.